iScience

CellPress
OPEN ACCESS

Article

Molecular convergence and transgenic evidence suggest a single origin of laryngeal echolocation in bats

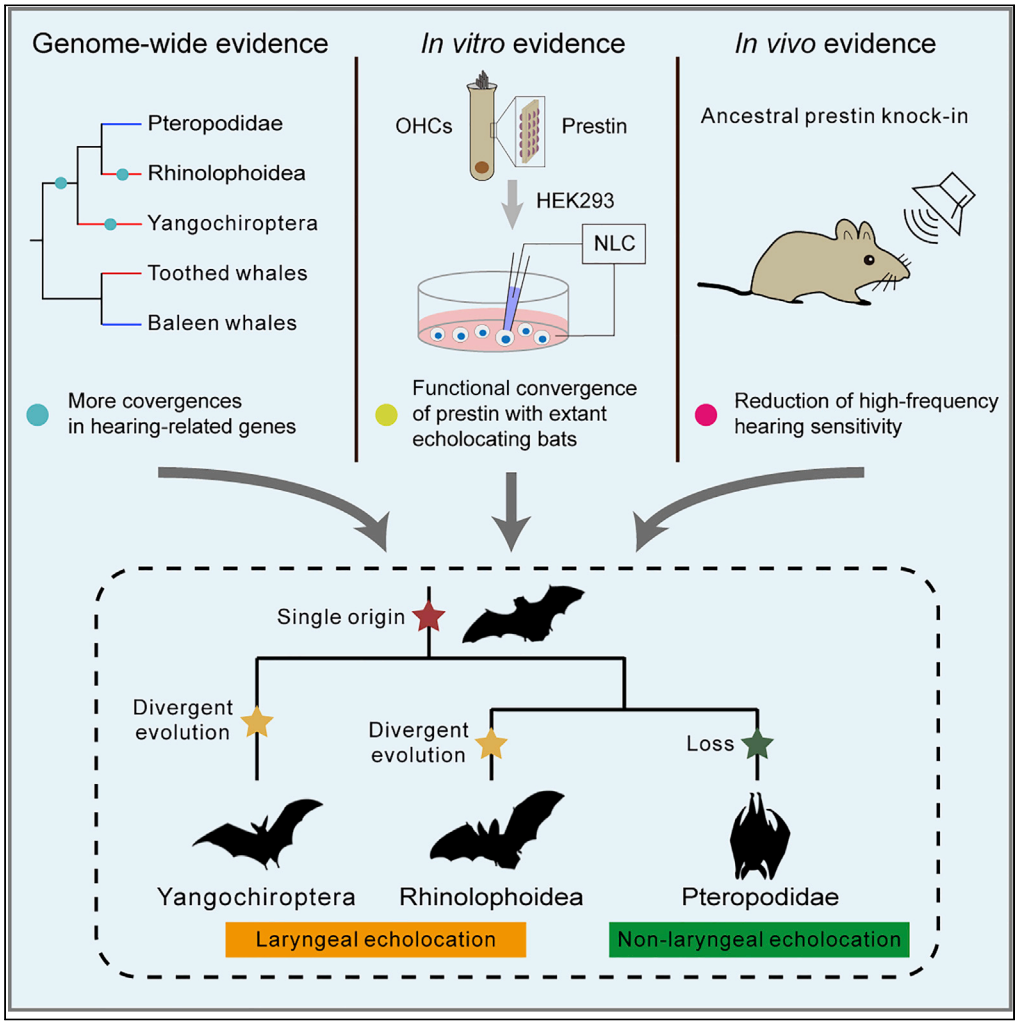

Zhen Liu, Peng Chen, Dong-Ming Xu, ..., Jing Bai, Xin Zhou, Peng Shi

ship@mail.kiz.ac.cn

Highlights

Convergences of bat common ancestor and toothed whales are enriched in hearing genes.

Natural selection drove convergences between bat common ancestor and toothed whales.

Prestin of bat common ancestor and extant echolocating bats functionally converges.

Two lines of transgenic mice suggest decreased hearing ability of fruit bat ancestor.

Liu et al., iScience *25*, 104114
April 15, 2022
https://doi.org/10.1016/j.isci.2022.104114

iScience

CellPress
OPEN ACCESS

Article

Molecular convergence and transgenic evidence suggest a single origin of laryngeal echolocation in bats

Zhen Liu,[1,5] Peng Chen,[1,2,5] Dong-Ming Xu,[1,5] Fei-Yan Qi,[1,5] Yuan-Ting Guo,[1,2] Qi Liu,[1,2] Jing Bai,[1,2] Xin Zhou,[1] and Peng Shi[1,3,4,6,*]

SUMMARY

The laryngeal echolocation is regarded as one of the conspicuous traits that play major roles in flourishing bats. Whether the laryngeal echolocation in bats originated once, however, is still controversial. We here address this question by performing molecular convergence analyses between ancestral branches of bats and toothed whales. Compared with controls, the molecular convergences were enriched in hearing-related genes for the last common ancestor of bats (LCAB) and extant echolocating bats, but not for the LCA of Old World fruit bats (LCAP). And the convergent hearing gene *prestin* of the LCAB and the extant echolocating bats functionally converged. More importantly, the high-frequency hearing of the LCAP-prestin knock-in mice decreased with lower cochlear outer hair cell function compared with the LCAB-prestin knock-in mice. Together, our findings provide multiple lines of evidence suggesting a single origin of laryngeal echolocation in the LCAB and the subsequent loss in the LCAP.

INTRODUCTION

Echolocation is an adaptive and perceptive behavior for obstacle avoidance, orientation, and hunting, which involves emitting sounds into the environment and listening to the echoes returning from objects (Jones, 2005). Although echolocation occurred in several mammalian lineages (He et al., 2021), its origin and elaboration have been widely studied only in bats and whales (Jones, 2005, 2010; Jones and Teeling, 2006). In contrast to a single origin of echolocation in the last common ancestor (LCA) of toothed whales supported by fossil records, molecular evolution, and gene functional experiments (Churchill et al., 2016; Geisler et al., 2014; Liu et al., 2018; Park et al., 2016), the evolutionary origin(s) of laryngeal echolocation in bats remain contentious (Jones and Teeling, 2006; Nojiri et al., 2021; Wang et al., 2017).

The phylogenetic relationship of bats reconstructed from extensive molecular data shows the laryngeally echolocating rhinolophoid bats and the nonecholocating pteropodid bats in the suborder Yinpterochiroptera, and other laryngeally echolocating bats in the suborder Yangochiroptera (Teeling et al., 2005; Tsagkogeorga et al., 2013), suggesting that the laryngeal echolocation either evolved in the LCA of bats (LCAB) and was subsequently lost in the LCA of pteropodids (LCAP) (Scenario 1), or evolved independently in echolocating bats from two suborders (Teeling et al., 2000, 2005). For the latter hypothesis, two derived scenarios were proposed depending on whether the LCAB echolocated (Nojiri et al., 2021). One scenario is that the LCAB was a non-echolocator and laryngeal echolocation completely independently evolved in two suborders (Scenario 2); the other scenario is that the LCAB was a primitive echolocator, and laryngeal echolocation was lost in pteropodids and evolved divergently in two suborders (Scenario 3) (Nojiri et al., 2021).

The currently discovered bat fossils suggest that laryngeal echolocation evolved in the ancestor of fossil bats (Simmons et al., 2008; Teeling, 2009), thus supporting Scenario 1. However, Scenarios two and three remain very hard to assess owing to the limited bat fossils, especially those with transitional morphological characters for laryngeal echolocation (Brown et al., 2019; Eiting and Gunnell, 2009; Teeling et al., 2005). A recent study indicates the developmental similarities of the inner ear between non-laryngeally echolocating bats (pteropodids) and non-bat mammals, and developmental dissimilarities of the inner ear and

[1]State Key Laboratory of Genetic Resources and Evolution, Kunming Institute of Zoology, Chinese Academy of Sciences, Kunming 650223, China

[2]University of Chinese Academy of Sciences, Beijing 100049, China

[3]School of Future Technology, University of Chinese Academy of Sciences, Beijing 100049, China

[4]Center for Excellence in Animal Evolution and Genetics, Chinese Academy of Sciences, Kunming 650223, China

[5]These authors contributed equally

[6]Lead contact

*Correspondence: ship@mail.kiz.ac.cn

https://doi.org/10.1016/j.isci.2022.104114

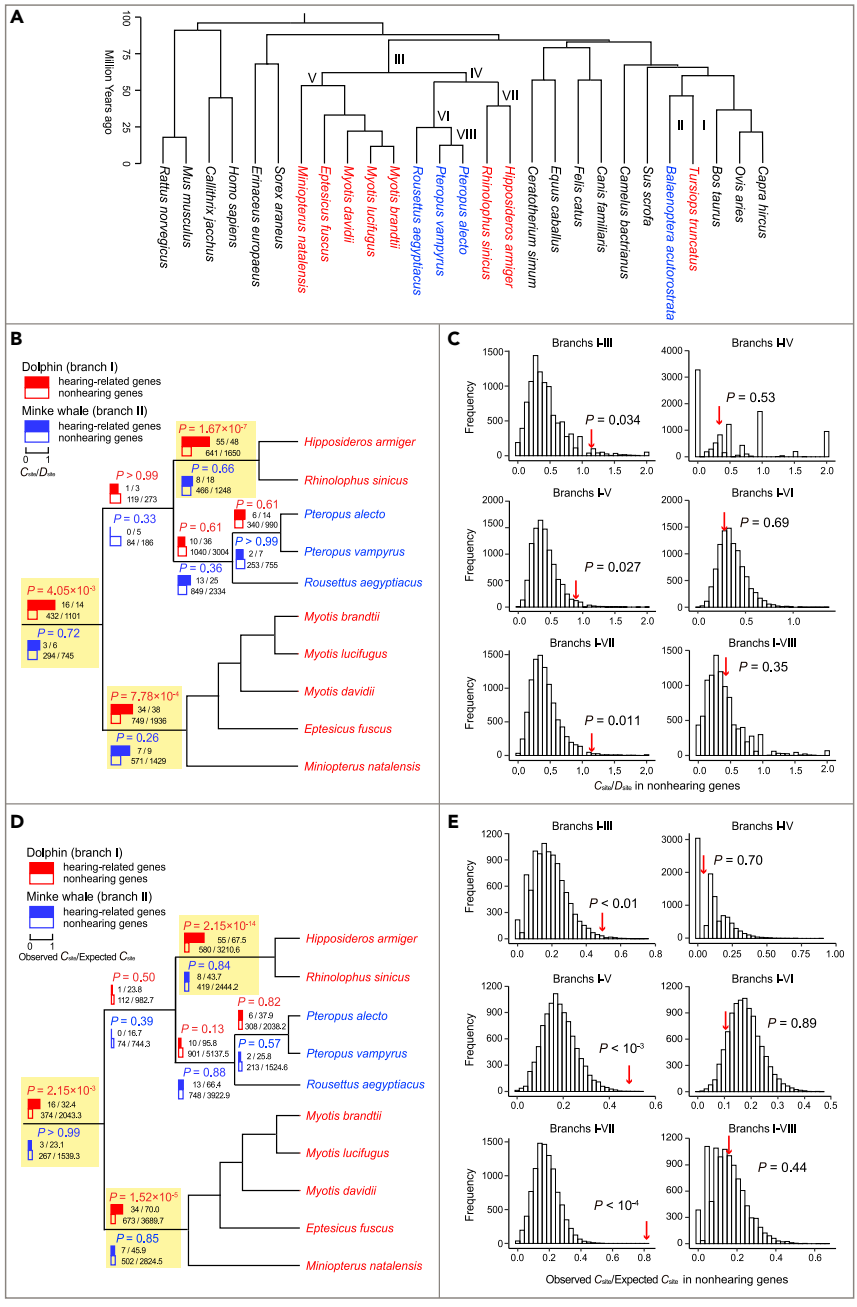

Figure 1. Genome-wide convergent analyses

(A) The phylogeny of 27 mammals used in this study. The red names highlight the laryngeally echolocating bats and the toothed whale, and the blue names their respective nonecholocating cohorts. The numbers I to VIII indicate the branches where convergent and divergent sites are counted.

(B) Comparisons for the ratios of the numbers of convergent sites to the number of divergent sites (C_{site}/D_{site}) in hearing-related and nonhearing genes between dolphin and different ancestral branches of bats, as well as between minke whale and different ancestral branches of bats.

(C) Frequency distributions of 1000 C_{site}/D_{site} values of 104 genes that are randomly picked from 11,041 nonhearing genes between dolphin and different ancestral branches of bats. The red arrow indicates the C_{site}/D_{site} value from 104 hearing-related genes for the branch pair in each panel.

(D) Comparisons for the ratios of the numbers of observed convergent sites to the number of expected convergent sites (observed C_{site}/expected C_{site}) in hearing-related and nonhearing genes between dolphin and different ancestral branches of bats, as well as between minke whale and different ancestral branches of bats.

Figure 1. *Continued*

(E) Frequency distributions of 1000 observed C_{site}/expected C_{site} values of 104 genes that are randomly picked from 11,041 nonhearing genes between dolphin and different ancestral branches of bats.

The red arrow indicates the observed C_{site}/expected C_{site} value from 104 hearing-related genes for the branch pair in each panel. The yellow boxes highlight statistically significant results. The *p* values on the branches are from two-tailed χ^2 tests.

stylohyal in the two laryngeally echolocating bats from Yinpterochiroptera and Yangochiroptera, supporting Scenarios two or 3 (Nojiri et al., 2021).

In contrast to the limited morphological characters with pervasive homoplasy on fossils (Zou and Zhang, 2016) and the developmental lability of characters (Levin, 1970), molecular data, such as DNA and protein sequences, can provide much information to elucidate the evolutionary histories of organisms and related traits (Nei and Kumar, 2000; Guo et al., 2021). Although toothed whales and laryngeally echolocating bats use very different forms of echolocation, they both need a high-frequency hearing to receive echoes (Jones, 2005, 2010). Indeed, several studies have shown more convergent (including parallel here) amino acid substitutions in hearing-related genes between laryngeally echolocating bats and toothed whales (Davies et al., 2011; Li et al., 2010; Liu et al., 2011, 2018; Parker et al., 2013; Shen et al., 2012). We thus proposed that if the laryngeal echolocation evolved in the LCAB and was subsequently lost in the LCAP, we would expect that (1) more convergences with toothed whales in the hearing-related genes is observed on the LCAB branch, not on the LCAP branch; (2) the function of convergent genes in the LCAB is similar to that of extant laryngeally echolocating bats, but different from that of the LCAP; and (3) the high-frequency hearing of the LCAP is reduced compared with the LCAB. In this study, we tested these predictions using evolutionary analyses of molecular convergence, functional experiments, and electrophysiological measurements of transgenic mice carrying ancestral genes.

RESULTS

More convergences in hearing-related genes between toothed whales and the LCAB suggest a single origin of laryngeal echolocation in bats

To investigate the molecular convergences between the LCAB and toothed whales, we obtained 11,145 one-to-one orthologous protein-coding genes across 27 mammals (Figure 1A), including seven laryngeally echolocating bats, three non-laryngeally echolocating pteropodid bats, one echolocating toothed whale (dolphin, *Tursiops truncatus*), and one nonecholocating baleen whale (minke whale, *Balaenoptera acutorostrata*). After inferring ancestral protein sequences for interior nodes using the maximum likelihood method (Yang, 2007), we identified 16 convergent sites in 15 of 104 hearing-related genes and 432 convergent sites in 408 of the remaining 11,041 nonhearing genes between dolphin (branch I) and the LCAB (branch III) (Tables S1, S2, and S3). The number of convergent sites (C_{site}) is shown to be proportional to the number of divergent sites (D_{site}) for a branch pair under no adaptive convergence (Castoe et al., 2009; Zou and Zhang, 2015b). For comparison, we also counted 14 and 1101 divergent sites for the hearing-related and nonhearing genes between the branches I and III (Tables S4 and S5). After controlling their respective numbers of divergent sites, the number of convergent sites in hearing-related genes significantly exceeded that in nonhearing genes between dolphin and the LCAB ($p = 0.0041$; two-tailed χ^2 test; Figure 1B). To confirm this result, we randomly picked the same number of nonhearing genes as that of hearing-related genes and counted C_{site} and D_{site} of these genes. After obtaining a null distribution of 1000 C_{site}/D_{site} values, we found that the C_{site}/D_{site} value of the hearing-related genes was, indeed, larger than those of nonhearing genes between dolphin and the LCAB ($p = 0.034$; Figure 1C). As controls, the above convergent analyses were performed between the LCAB and the nonecholocating minke whale (branch II) that is phylogenetically equally close to dolphin, as well as between the LCAB and cow (branch II′) that is phylogenetically distant from dolphin. We found no more convergences in the hearing-related genes than in nonhearing genes for all of the comparisons between the minke whale and the LCAB, and between cow and the LCAB ($p > 0.2$; Figures 1B, S1A, and S2; Tables S1–S5).

Next, we tested whether more convergences in hearing-related genes between the LCAB and dolphin were driven by natural selection. If this is true, the ratio of the number of observed convergent sites (observed C_{site}) to the number of expected convergent sites (expected C_{site}) under neutral evolutionary models should be larger in hearing-related genes than in nonhearing genes. To test this prediction, we, respectively, estimated the expected C_{site} values for the hearing-related and nonhearing genes between dolphin and the LCAB under the neutral evolutionary models (Zou and Zhang, 2015a). Indeed, the value

of observed C_{site}/expected C_{site} was significantly larger in hearing-related genes than in nonhearing genes ($p = 0.0022$; two-tailed χ^2 test; Figure 1D). This result was further confirmed by subsampling the same number of nonhearing genes as that of the hearing-related genes to perform the evolutionary analyses above ($p < 0.01$; Figure 1E). The same evolutionary analyses were also performed between the LCAB and the minke whale, as well as between the LCAB and cow, but no significant differences in the observed C_{site}/expected C_{site} values were found between the hearing-related and nonhearing genes ($p > 0.2$; Figures 1D, 1E, S1B, and S2).

Laryngeal echolocation divergently evolved in the LCA of extant echolocating bats and lost in the LCA of Old World fruit bats

To test whether laryngeal echolocation divergently evolved in the yinpterochiropteran and yangochiropteran bats, we performed the above convergent evolution analyses between dolphin (branch I) and the LCAs of other bat clades, including yinpterochiropteran bats (branch IV), yangochiropteran bats (branch V), pteropodid bats (branch VI), rhinolophoid bats (branch VII), and Pteropus bats (branch VIII) (Figure 1A). As in the LCAB, we observed more convergences in the hearing-related genes between dolphin and the LCAs of the laryngeally echolocating yangochiropteran and rhinolophoid bats (Figures 1B and 1C; Tables S2 and S3). By contrast, no more convergences were found in hearing-related genes between dolphin and the LCAP, as well as between dolphin and the LCA of Pteropus bats (LCAPT; Figures 1B and 1C; Tables S2 and S3). As controls, we also conducted the same convergent evolutionary analyses between these LCAs of bat clades and the minke whale, as well as between these LCAs of bat clades and cow. No more convergences in the hearing-related genes than in nonhearing genes were found for all of the comparisons (Figures 1B, S1A, and S2; Tables S2–S5).

We also tested for natural selection on the convergences in hearing-related genes between dolphin and the LCAs of different bat clades using the neutral expectations above. The observed C_{site}/expected C_{site} values were significantly larger in hearing-related genes than in nonhearing genes on the ancestral branches leading to the laryngeally echolocating yangochiropteran bats and rhinolophoid bats, but not on the ancestral branches leading to pteropodid bats and Pteropus bats (Figures 1D and 1E). As controls, the above evolutionary evolution analyses were also performed between the minke whale and these LCAs of bats, as well as between cow and these LCAs of bats. No significant differences in the observed C_{site}/expected C_{site} values were found in all comparisons between the hearing-related and nonhearing genes (Figures 1D, 1E, S1B, and S2).

Functional convergence of echolocation-related gene *prestin* between the LCAB and extant echolocating bats

Interestingly, we found that the echolocation-related hearing gene *prestin* (also known as *SLC26A5*) had a convergent amino acid (L497M) between the LCAB and dolphin (Table S2). Also, several previous studies showed significant convergences in the prestin sequences between echolocating bats and toothed whales (Li et al., 2010; Liu et al., 2010, 2014, 2018). And the identified convergent sites are largely responsible for the functional convergence of a higher $1/\alpha$ parameter of prestin between echolocating mammals, which exhibits a significantly positive correlation with the high-frequency hearing (Liu et al., 2014, 2018). More interestingly, prestin carrying the convergent substitutions from echolocating mammals is more sensitive for high-frequency sounds (Huang et al., 2020). Accordingly, we hypothesized that if the LCAB evolved echolocation, the LCAB prestin should function like that of the extant laryngeally echolocating bats, rather than that of the nonecholocating pteropodid bats. To test this hypothesis, we inferred and synthesized the LCAB *prestin* sequence based on a phylogeny of 40 mammals (Figure 2A) and performed the functional analyses using the whole-cell patch-clamp recording (Schaechinger et al., 2011). The nonlinear capacitance (NLC) of positive cells transfected by the LCAB *prestin* was measured and displayed a robust bell-shaped dependence on membrane potential (Figure 2B), indicating a great functionality of the ancestry gene. We focused on the functional parameter $1/\alpha$ of prestin because it decreases in cells from the more basal cochlea that is sensitive to high-frequency sounds (Ashmore, 1987; Santos-Sacchi et al., 1998), its values significantly correlate with best-frequency hearing across mammals (Liu et al., 2018), and its significant convergence between echolocating mammals (Liu et al., 2014). The functional parameter $1/\alpha$ (59.6 ± 13.8 mV) of the LCAB prestin was larger than that from the nonecholocating pteropodid bat *Cynopterus sphinx* ($p = 1.22 \times 10^{-7}$, two-tailed Student's *t* test; Figure 2C), as observed in the extant laryngeally echolocating bats, such as *Aselliscus stoliczkanus*, *Megaderma lyra*, and *Myotis ricketti* (Liu et al., 2014, 2018).

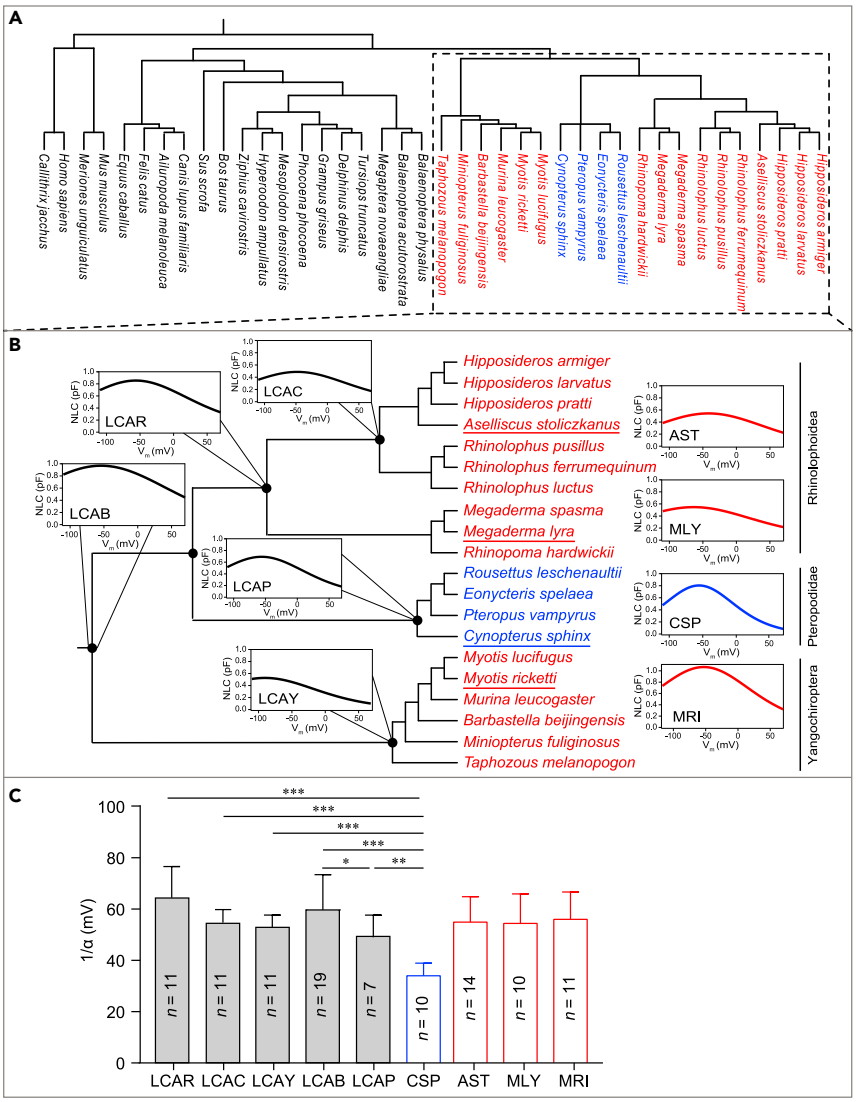

Figure 2. Functional tests of the resurrected *prestin* genes from different ancestral bats

(A) A phylogeny across 40 mammals used to infer ancestral prestin sequences. The red names denote laryngeally echolocating bats and the blue ones fruit bats.

(B) Schematic phylogenetic tree showing how the function of prestin changes among different bat ancestors. The functional data of *prestin* genes from living bats marked by underlines are modified from Liu et al. (2014) and (2018). Representative fitting curves of NLC derived from the examined *prestin* genes are shown.

(C) Comparison of the functional parameter 1/α values of prestin among the ancestral and living bats. As the extant laryngeally echolocating bats including *Aselliscus stoliczkanus* (denoted as AST for short), *Megaderma lyra* (MLY), and *Myotis ricketti* (MRI), the 1/α value of prestin significantly increases in the ancestral bats including LCAB, LCAY, LCAR, LCAP, and LCAC compared with the living nonecholocating bat *Cynopterus sphinx* (CSP). Among ancestral bats, the 1/α of prestin is significantly smaller for the LCAP than for the LCAB. The values of *n* represent numbers of cells.

Data are represented as mean $\pm$ SD *p < 0.05, **p < 0.01, ***p < 0.001. All *p* values are from two-tailed Student's *t*-tests.

To further explore how *prestin* functionally changed during bat evolution, we inferred the *prestin* sequences from the key evolutionary nodes of bats, including the last common ancestors of yangochiropteran bats (LCAY), yinpterochiropteran bats, rhinolophoid bats (LCAR), pteropodid bats (LCAP), and rhinolophid bats (LCAC). Of these, the inferred *prestin* sequence of the ancestor of yinpterochiropteran bats was identical to the LCAB *prestin*. After synthesizing these ancestral *prestin* sequences, we performed the functional analyses and found that all of these ancestral genes exhibited bell-shaped NLC curves similar to those of extant bats (Figure 2B). As the extant laryngeally echolocating bats and the LCAB, the prestin

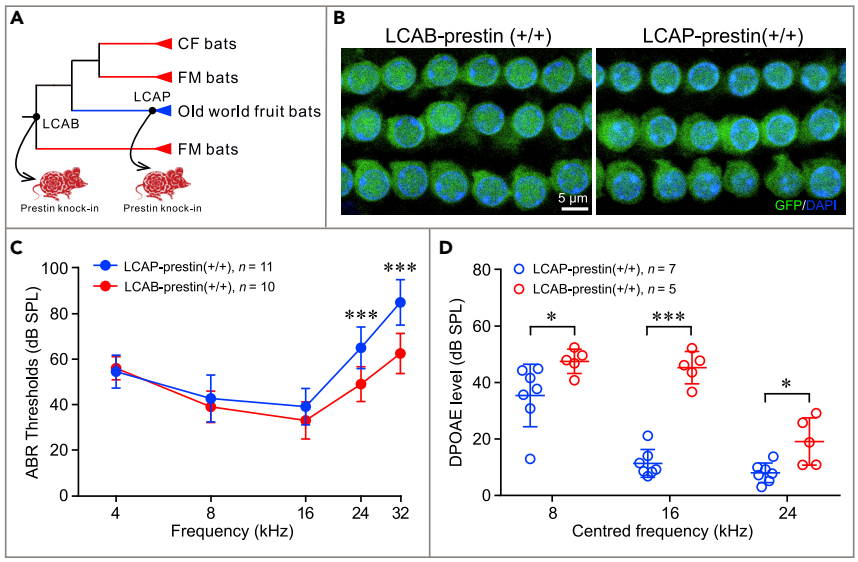

Figure 3. Auditory tests for the LCAB-prestin and LCAP-prestin knock-in mice

(A) A simplified phylogenetic tree showing the nodes of the LCAB and LCAP to create the transgenic mice.

(B) Representative confocal microscopy images of GFP-positive OHCs at the basal turn of cochlear for the LCAB-prestin and LCAP-prestin knock-in mice.

(C) The ABR thresholds at the high frequencies of 24 and 32 kHz are significantly reduced in the LCAP-prestin knock-in mice compared with the LCAB-prestin knock-in mice.

(D) Average DPOAE levels at the centered frequencies generally are significantly smaller for the LCAP-prestin knock-in mice than for the LCAB-prestin knock-in mice.

The values of *n* indicate the numbers of biologically independent animals. All data are denoted as mean ± SD All *p* values are from two-tailed Student's *t*-tests. *p < 0.05, ***p < 0.001.

1/α values of the LCAY, LCAR, LCAP, and LCAC were significantly larger than that of the nonecholocating pteropodid bat *C. sphinx* (p < 0.01, two-tailed Student *t*-tests; Figure 2C). These results suggest that the LCAB, as well as other bat ancestors, have evolved the high-frequency hearing compared with the extant nonecholocating bats.

The reduced high-frequency hearing of the LCAP-prestin knock-in mice compared with the LCAB-prestin knock-in mice

Notably, despite generally larger 1/α values of the ancestral prestins than the extant nonecholocating bat, the 1/α value was significantly smaller for the LCAP prestin than for the LCAB prestin (p = 0.032; two-tailed Student's *t* test; Figure 2C), suggesting a weaker high-frequency hearing of the LCAP than the LCAB. To test this suggestion, we generated two lines of transgenic mice carrying the LCAP *prestin* and LCAB *prestin*, respectively (Figure 3A). An EGFP reporter was inserted downstream of *prestin*, separated by an IRES sequence. As indicated by GFP, the LCAB and LCAP prestins were normally and almost indistinguishably expressed in the cochlear outer hair cells (OHCs) in two transgenic mice (Figure 3B). To examine the influences of the LCAB and LCAP prestins on hearing, we, respectively, measured their auditory brainstem responses (ABRs). At the low frequencies of 4, 6, and 16 kHz, the ABR thresholds in the LCAP-prestin knock-in mice were virtually identical to those in the LCAB-prestin knock-in mice (p > 0.05; two-tailed Student's *t* test; Figure 3C). However, the ABR thresholds were significantly higher in the LCAP-prestin knock-in mice than in the LCAB-prestin knock-in mice at the examined high frequencies of 24 and 32 kHz (p < 0.001; two-tailed Student's *t*-tests; Figure 3C).

While ABRs reflect the summed activity of the neural output of the cochleae, the distortion product otoacoustic emissions (DPOAEs) are generated presynaptically, depending critically only on the normal function of the OHCs. Given that prestin functions in the OHCs as a motor protein (Zheng et al., 2000), we thus performed DPOAE tests for the LCAB- and LCAP-prestin knock-in mice by using frequency-specific tone-burst stimuli centered around the frequencies of 8, 16, and 24 kHz. We found that the LCAP-prestin knock-in mice displayed significantly reduced DPOAE responses at all examined stimulus frequencies

compared with the LCAB-prestin knock-in mice ($p < 0.05$; two-tailed Student's *t* test; Figure 3D). These results demonstrate the lower OHC function in the LCAP-prestin knock-in mice than in the LCAB-prestin knock-in mice. Collectively, the acoustic characteristics of the transgenic mice carrying the ancestral echolocation-related gene *prestin* indicate the reduced high-frequency hearing and lower OHC function for the LCAP-prestin knock-in mice than for the LCAB-prestin knock-in mice, suggesting that the high-frequency hearing is subsequently relaxed in the LCAP as it originated in the LCAB.

DISCUSSION

As molecular data support the paraphyletic relationship of laryngeally echolocating bats, it has been argued that the laryngeal echolocation either evolved in the LCAB and was subsequently lost in the LCAP (Scenario 1), or evolved independently in the LCAR and the LCAY (Scenario 2), or evolved in the LCAB as a primitive form, was lost in the LCAP, and divergently evolved in the LCAR and the LCAY (Scenario 3) (Nojiri et al., 2021; Teeling et al., 2000, 2005; Tsagkogeorga et al., 2013). The limited bat fossil records, particularly missing those with transitional morphological adaptations, impede the understanding of the origin and development of laryngeal echolocation in bats (Teeling et al., 2005). An alternative strategy for addressing this question is to examine the evolutionary patterns of the genes related to echolocation (Liu et al., 2018; Teeling, 2009). In this study, more convergences in the hearing-related genes between the LCAB and the toothed whale, as well as the functional convergence of the echolocation-related *prestin* between the LCAB and extant laryngeally echolocating bats, suggest a single origin of laryngeal echolocation in the LCAB. Similar results were also observed on the ancestral branches leading to the extant laryngeally echolocating bats, suggesting that after emergence, laryngeal echolocation further divergently evolved. Notably, our results are limited to determining whether the laryngeal echolocation evolved in the LCAB is primitive or not, thus supporting Scenarios one and 3.

The reliability of the convergent analyses on protein-coding gene sequences primarily relies on the accuracy of ancestral reconstructions. Although the maximum likelihood approach was used in the above convergent analyses because of its pros in dealing with distantly related sequences and complex configuration of amino acids, it may bias against detecting the convergence that occurs on short branches, such as the stem Yangochiroptera and stem Yinpterochiroptera branches (Nei and Kumar, 2000). By contrast, the maximum parsimony method is effective in inferring ancestral sequences when the divergence of extant sequences is low (Nei and Kumar, 2000). Thus, to confirm the results of our convergent analyses, we reanalyzed our data by using the maximum parsimony method to infer ancestral sequences (Yang, 2007). The results were very similar to those based on the maximum likelihood ancestral reconstructions, further supporting our conclusion (Figure S3; Tables S6–S9).

It is of note that these results from evolutionary analyses may be biased by a small sample size of only containing a single toothed whale. To overcome this potential limitation, we collected 10,866 one-to-one orthologous protein-coding genes across 116 mammalian species including at least four toothed whales to perform convergent evolution analyses (Figure S4A). Similar to the dataset of 27 mammals, more convergences with toothed whales in the hearing-related genes were observed on the ancestral branches of all bats and two groups of the laryngeally echolocating yangochiropteran bats and rhinolophoid bats, but not on the ancestral branches of nonecholocating Old World fruit bats (Figures S4B and S4C; Tables S10–S13). In addition, no more convergences with toothed whales in the hearing-related genes were observed on the ancestral branch of the yinpterochiropteran bats (branch IV) and the *prestin* sequence of the ancestor of yinpterochiropteran bats was inferred to be identical with that of the LCAB. These results might result from a relatively short evolutionary time of the yinpterochiropteran ancestor (Teeling et al., 2005), although they could be challenged as the number of bat species involved in the analyses increases.

Many molecular studies on bat echolocation suggest that the laryngeal echolocation evolved independently in the LCAR and the LCAY. For example, molecular convergences were found in at least seven hearing-related genes *prestin*, *KCNQ4*, *CDH23*, *PCDH15*, *OTOF*, *TMC1*, and *PJVK* among the LCAR, the LCAY, and toothed whales (Davies et al., 2011; Li et al., 2008, 2010; Liu et al., 2010, 2011; Shen et al., 2012), which, however, do not necessarily preclude Scenario one that the laryngeal echolocation evolved in the LCAB. On the one hand, given various forms of echolocation calls in bats, it is reasonable to assume that echolocation divergently evolved (Scenarios two and 3) after its origin during the evolution of bats (Jones and Teeling, 2006). The observation of molecular convergences among the LCAR, the LCAY, and toothed

whales probably reflect the subsequent evolutionary pattern of echolocation, rather than its origin. On the other hand, echolocation is a complex system, showing many phenotypical specializations associated with sound production, hearing, and neural processing. Of the hundreds of the genes underlying these echolocation-related phenotypes, case studies are largely impotent in discerning which genes are involved in the origin of echolocation, or the elaboration of echolocation, or both.

Based on the molecular phylogeny of bats, a single origin of laryngeal echolocation in the LCAB suggests that the LCAP either lost the laryngeal echolocation or retained some vestigial characters of the rudimentary echolocation (Teeling et al., 2000, 2005). Although we observed no more convergences with toothed whales in the hearing-related genes on the branch of the LCAP, it is not indicative of relaxed selection in the hearing-related genes. Accordingly, we examined signals of the relaxed selection in the hearing-related genes along the branch of the LCAP and identified six genes under the relaxed selection (Table S14). Interestingly, the hearing-related gene *TMC1*, which was under convergent evolution with dolphin on the ancestral branches of echolocating yangochiropteran bats and rhinolophoid bats, was relaxed on the branch of the LCAP (selection intensity parameter $K = 0$; $p = 0.013$). Compared with the transgenic mice carrying the LCAB *prestin*, the reduced high-frequency hearing and lower OHC function in the transgenic mice carrying the LCAP *prestin* suggest that the high-frequency hearing, indeed, degenerated in the LCAP. Nevertheless, our functional analyses of the echolocation-related gene *prestin* exhibited a higher $1/\alpha$ value in the LCAP than in the extant fruit bat (Figure 2C), as is observed between echolocating and nonecholocating mammals (Liu et al., 2014, 2018), suggesting that the LCAP retained some vestigial ability of relatively high-frequency hearing. Notably, some nonecholocating fruit bats were reported to produce sonar sounds with tongue clicks or wing claps (Boonman et al., 2014), which substantially differ from laryngeal echolocation.

Besides fossils and molecular evolution, the developmental patterns of echolocation-related traits, such as inner ears and stylohyoid bones, are also used to investigate the origin of laryngeal echolocation in bats. However, owing to the limited sampling of bat species for prenatal stages, the skewed developmental stages between species, and the evolutionary liability of prenatal skeleton development (Hirasawa and Kuratani, 2015; Nojiri et al., 2018; Pennisi, 1997), different studies provided contrast evidence for the origin of laryngeal echolocation in bats. For example, a previous study showed that the cochlear growth rate of the pteropodid bat is similar to the laryngeally echolocating bats in prenatal development, but slows later in development, supporting scenario one of a single origin of laryngeal echolocation in the LCAB (Wang et al., 2017). By contrast, another study revealed different developmental patterns of inner ears and the stylohyal between the echolocating yangochiropteran bats and rhinolophid bats, supporting Scenarios two and 3. Our study represents an alternative, systematic strategy to resolve a long-standing evolutionary dispute in bat biology by incorporating genome-wide convergence analyses, functional experiments by resurrecting ancestral genes, and physiological measurements of transgenic mice.

Limitations of the study

Our convergent evolution analyses at the genomic scale only focused on the same sites of the same sets of protein-coding genes in the evolution of echolocation between different groups of bats and cetaceans, which largely takes no account of different genetic routes involved in the evolution of echolocation as suggested in the previous studies (Nojiri et al., 2021; Sulser et al., 2022). In fact, there are no effective approaches or testable hypotheses for determining the diversified molecular bases associated with convergent phenotypes to date, and it is a major challenge for any study exploring genomic changes underlying macroevolutionary traits to distinguish between causal genomic changes that directly contributed to these traits and secondary changes that occurred after these traits evolved (Stern, 2013). Despite the limitation, our comparative genomic analyses, particularly combined with the functional experiments *in vitro* and *in vivo*, highlight a promising evolutionary trajectory of echolocation in bats.

STAR★METHODS

Detailed methods are provided in the online version of this paper and include the following:

- KEY RESOURCES TABLE
- RESOURCE AVAILABILITY
  - Lead contact
  - Materials availability

SUPPLEMENTAL INFORMATION

Supplemental information can be found online at https://doi.org/10.1016/j.isci.2022.104114.

ACKNOWLEDGMENTS

We thank Hui Yang for the valuable comments. This work was supported by grants from the National Natural Science Foundation of China (31922010, 31930011, 31871270, 32192422), the Strategic Priority Research Program of the Chinese Academy of Sciences (XDPB17), National Key Research and Development Program of China (2021YFC2301300), the Key Research Program of the Chinese Academy of Sciences (KJZD-SW-L11), the Yunnan Provincial Science and Technology Department (2019FI008), and the Major Science and Technique Programs in Yunnan Province (202102AA310055).

AUTHOR CONTRIBUTIONS

The project was supervised and originally designed by Z.L. and P.S.. D.M.X. and Y.T.G analyzed genome-wide molecular convergences and inferred ancestral sequences; P.C., Q.L., and J.B. performed animal experiments and acoustic recordings; F.Y.Q. and X.Z. cultured cells and conducted electrophysiological experiments; the article was written by Z.L., P.C., and P.S.

DECLARATION OF INTERESTS

The authors declare no competing interests.

Received: August 7, 2020
Revised: March 7, 2022
Accepted: March 15, 2022
Published: April 15, 2022

REFERENCES

Ashmore, J.F. (1987). A fast motile response in Guinea-pig outer hair cells: the cellular basis of the cochlear amplifier. J. Physiol. *388*, 323–347. https://doi.org/10.1113/jphysiol.1987.sp016617.

Boonman, A., Bumrungsri, S., and Yovel, Y. (2014). Nonecholocating fruit bats produce biosonar clicks with their wings. Curr. Biol. *24*, 2962–2967. https://doi.org/10.1016/j.cub.2014.10.077.

Brown, E.E., Cashmore, D.D., Simmons, N.B., Butler, R.J., and Mannion, P. (2019). Quantifying the completeness of the bat fossil record. Palaeontology *62*, 757–776. https://doi.org/10.1111/pala.12426.

Castoe, T.A., de Koning, A.P., Kim, H.M., Gu, W., Noonan, B.P., Naylor, G., Jiang, Z.J., Parkinson, C.L., and Pollock, D.D. (2009). Evidence for an ancient adaptive episode of convergent molecular evolution. Proc. Natl. Acad. Sci. U S A *106*, 8986–8991. https://doi.org/10.1073/pnas.0900233106.

Churchill, M., Martinez-Caceres, M., de Muizon, C., Mnieckowski, J., and Geisler, J.H. (2016). The origin of high-frequency hearing in whales. Curr. Biol. *26*, 2144–2149. https://doi.org/10.1016/j.cub.2016.06.004.

Davies, K.T., Cotton, J.A., Kirwan, J.D., Teeling, E.C., and Rossiter, S.J. (2011). Parallel signatures of sequence evolution among hearing genes in echolocating mammals: an emerging model of genetic convergence. Heredity (Edinb) *108*, 480–489. https://doi.org/10.1038/hdy.2011.119.

Eiting, T.P., and Gunnell, G.F. (2009). Global completeness of the bat fossil record. J. Mamm. Evol. *16*, 151–173. https://doi.org/10.1007/s10914-009-9118-x.

Geisler, J.H., Colbert, M.W., and Carew, J.L. (2014). A new fossil species supports an early origin for toothed whale echolocation. Nature *508*, 383–386. https://doi.org/10.1038/nature13086.

Guo, Y.T., Zhang, J., Xu, D.M., Tang, L.T., and Liu, Z. (2021). Phylogenomic relationships and molecular convergences to subterranean life in rodent family spalacidae. Zool. Res. *42*, 671–674. https://doi.org/10.24272/j.issn.2095-8137.2021.240.

He, K., Liu, Q., Xu, D.M., Qi, F.Y., Bai, J., He, S.W., Chen, P., Zhou, X., Cai, W.Z., Chen, Z.Z., et al.

(2021). Echolocation in soft-furred tree mice. Science *372*, eaay1513. https://doi.org/10.1126/science.aay1513.

Hirasawa, T., and Kuratani, S. (2015). Evolution of the vertebrate skeleton: morphology, embryology, and development. Zool. Lett. *1*, 2. https://doi.org/10.1186/s40851-014-0007-7.

Huang, Y.S., Fan, C.H., Hsu, N., Chiu, N.H., Wu, C.Y., Chang, C.Y., Wu, B.H., Hong, S.R., Chang, Y.C., Yan-Tang Wu, A., et al. (2020). Sonogenetic modulation of cellular activities using an engineered auditory-sensing protein. Nano Lett. *20*, 1089–1100. https://doi.org/10.1021/acs.nanolett.9b04373.

Jones, G. (2005). Echolocation. Curr. Biol. *15*, R484–R488. https://doi.org/10.1016/j.cub.2005.06.051.

Jones, G. (2010). Molecular evolution: gene convergence in echolocating mammals. Curr. Biol. *20*, R62–R64. https://doi.org/10.1016/j.cub.2009.11.059.

Jones, G., and Teeling, E.C. (2006). The evolution of echolocation in bats. Trends Ecol. Evol. *21*, 149–156. https://doi.org/10.1016/j.tree.2006.01.001.

Levin, D.A. (1970). Developmental instability and evolution in peripheral isolates. Am. Nat. *104*, 343–353. https://doi.org/10.1086/282668.

Li, G., Wang, J., Rossiter, S.J., Jones, G., Cotton, J.A., and Zhang, S. (2008). The hearing gene Prestin reunites echolocating bats. Proc. Natl. Acad. Sci. U S A *105*, 13959–13964. https://doi.org/10.1073/pnas.0802097105.

Li, Y., Liu, Z., Shi, P., and Zhang, J. (2010). The hearing gene Prestin unites echolocating bats and whales. Curr. Biol. *20*, R55–R56. https://doi.org/10.1016/j.cub.2009.11.042.

Liu, Y., Cotton, J.A., Shen, B., Han, X., Rossiter, S.J., and Zhang, S. (2010). Convergent sequence evolution between echolocating bats and dolphins. Curr. Biol. *20*, R53–R54. https://doi.org/10.1016/j.cub.2009.11.058.

Liu, Z., Li, S., Wang, W., Xu, D., Murphy, R.W., and Shi, P. (2011). Parallel evolution of KCNQ4 in echolocating bats. PLoS One *6*, e26618. https://doi.org/10.1371/journal.pone.0026618.

Liu, Z., Qi, F.Y., Xu, D.M., Zhou, X., and Shi, P. (2018). Genomic and functional evidence reveals molecular insights into the origin of echolocation in whales. Sci. Adv. *4*, eaat8821. https://doi.org/10.1126/sciadv.aat8821.

Liu, Z., Qi, F.Y., Zhou, X., Ren, H.Q., and Shi, P. (2014). Parallel sites implicate functional convergence of the hearing gene prestin among echolocating mammals. Mol. Biol. Evol. *31*, 2415–2424. https://doi.org/10.1093/molbev/msu194.

Nei, M., and Kumar, S. (2000). Molecular Evolution and Phylogenetics (Oxford University Press).

Nojiri, T., Werneburg, I., Son, N.T., Tu, V.T., Sasaki, T., Maekawa, Y., and Koyabu, D. (2018). Prenatal cranial bone development of Thomas's horseshoe bat (Rhinolophus thomasi): with special reference to petrosal morphology. J. Morphol. *279*, 809–827. https://doi.org/10.1002/jmor.20813.

Nojiri, T., Wilson, L.A.B., pez-Aguirre, C.L., Tu, V.T., Kuratani, S., Ito, K., Higashiyama, H., Son, N.T., Fukui, D., Sadier, A., et al. (2021). Embryonic evidence uncovers convergent origins of laryngeal echolocation in bats. Curr. Biol. *31*, 1–13. https://doi.org/10.1016/j.cub.2020.12.043.

Park, T., Fitzgerald, E.M., and Evans, A.R. (2016). Ultrasonic hearing and echolocation in the earliest toothed whales. Biol. Lett. *12*, 20160060. https://doi.org/10.1098/rsbl.2016.0060.

Parker, J., Tsagkogeorga, G., Cotton, J.A., Liu, Y., Provero, P., Stupka, E., and Rossiter, S.J. (2013). Genome-wide signatures of convergent evolution in echolocating mammals. Nature *502*, 228–231. https://doi.org/10.1038/nature12511.

Pennisi, E. (1997). Haeckel's embryos: fraud rediscovered. Science *277*, 1435. https://doi.org/10.1126/science.277.5331.1435a.

Santos-Sacchi, J., Kakehata, S., Kikuchi, T., Katori, Y., and Takasaka, T. (1998). Density of motility-related charge in the outer hair cell of the Guinea pig is inversely related to best frequency. Neurosci. Lett. *256*, 155–158. https://doi.org/10.1016/s0304-3940(98)00788-5.

Schaechinger, T.J., Gorbunov, D., Halaszovich, C.R., Moser, T., Kugler, S., Fakler, B., and Oliver, D. (2011). A synthetic prestin reveals protein domains and molecular operation of outer hair cell piezoelectricity. EMBO J. *30*, 2793–2804. https://doi.org/10.1038/emboj.2011.202.

Scornavacca, C., Belkhir, K., Lopez, J., Dernat, R., Delsuc, F., Douzery, E.J.P., and Ranwez, V. (2019). OrthoMaM v10: scaling-up orthologous coding sequence and exon alignments with more than one hundred Mammalian genomes. Mol. Biol. Evol. *36*, 861–862. https://doi.org/10.1093/molbev/msz015.

Shen, Y.Y., Liang, L., Li, G.S., Murphy, R.W., and Zhang, Y.P. (2012). Parallel evolution of auditory genes for echolocation in bats and toothed whales. PLoS Genet. *8*, e1002788. https://doi.org/10.1371/journal.pgen.1002788.

Simmons, N.B., Seymour, K.L., Habersetzer, J., and Gunnell, G.F. (2008). Primitive early Eocene bat from Wyoming and the evolution of flight and echolocation. Nature *451*, 818–821. https://doi.org/10.1038/nature06549.

Stern, D.L. (2013). The genetic causes of convergent evolution. Nat. Rev. Genet. *14*, 751–764. https://doi.org/10.1038/nrg3483.

Sulser, R.B., Patterson, B.D., Urban, D.J., Neander, A.I., and Luo, Z.X. (2022). Evolution of inner ear neuroanatomy of bats and implications for echolocation. Nature *602*, 449–454. https://doi.org/10.1038/s41586-021-04335-z.

Teeling, E.C. (2009). Hear, hear: the convergent evolution of echolocation in bats? Trends Ecol. Evol. *24*, 351–354. https://doi.org/10.1016/j.tree.2009.02.012.

Teeling, E.C., Scally, M., Kao, D.J., Romagnoli, M.L., Springer, M.S., and Stanhope, M.J. (2000). Molecular evidence regarding the origin of echolocation and flight in bats. Nature *403*, 188–192. https://doi.org/10.1038/35003188.

Teeling, E.C., Springer, M.S., Madsen, O., Bates, P., O'Brien S, J., and Murphy, W.J. (2005). A molecular phylogeny for bats illuminates biogeography and the fossil record. Science *307*, 580–584. https://doi.org/10.1126/science.1105113.

Tsagkogeorga, G., Parker, J., Stupka, E., Cotton, J.A., and Rossiter, S.J. (2013). Phylogenomic analyses elucidate the evolutionary relationships of bats. Curr. Biol. *23*, 2262–2267. https://doi.org/10.1016/j.cub.2013.09.014.

Wang, Z., Zhu, T., Xue, H., Fang, N., Zhang, J., Zhang, L., Pang, J., Teeling, E.C., and Zhang, S. (2017). Prenatal development supports a single origin of laryngeal echolocation in bats. Nat. Ecol. Evol. *1*, 21. https://doi.org/10.1038/s41559-016-0021.

Yang, Z. (2007). PAML 4: phylogenetic analysis by maximum likelihood. Mol. Biol. Evol. *24*, 1586–1591. https://doi.org/10.1093/molbev/msm088.

Zheng, J., Shen, W., He, D.Z., Long, K.B., Madison, L.D., and Dallos, P. (2000). Prestin is the motor protein of cochlear outer hair cells. Nature *405*, 149–155. https://doi.org/10.1038/35012009.

Zou, Z., and Zhang, J. (2015a). Are convergent and parallel amino acid substitutions in protein evolution more prevalent than neutral expectations? Mol. Biol. Evol. *32*, 2085–2096. https://doi.org/10.1093/molbev/msv091.

Zou, Z., and Zhang, J. (2016). Morphological and molecular convergences in mammalian phylogenetics. Nat. Commun. *7*, 12758. https://doi.org/10.1038/ncomms12758.

Zou, Z.T., and Zhang, J.Z. (2015b). No genome-wide protein sequence convergence for echolocation. Mol. Biol. Evol. *32*, 1237–1241. https://doi.org/10.1093/molbev/msv014.

STAR★METHODS

KEY RESOURCES TABLE

REAGENT or RESOURCE	SOURCE	IDENTIFIER
Chemicals, peptides, and recombinant proteins		
CsCl	Sigma-Aldrich	289329
$MgCl_2$	Sigma-Aldrich	M8266
NaCl	Sigma-Aldrich	S9888
$CoCl_2$	Sigma-Aldrich	232696
TEA-Cl	Sigma-Aldrich	T2265
EGTA	Sigma-Aldrich	E3889
HEPES	Sigma-Aldrich	H3375
Glucose	Sigma-Aldrich	D8270
EDTA	Sigma-Aldrich	E9884
Lipofectamine 2000 transfection reagent	Invitrogen	11668019
Antifading mountant medium with DAPI	Solarbio	S2110
Deposited data		
protein alignments	OrthoMaM database	v10b
Experimental models: Cell lines		
HEK293	This lab	N/A
Experimental models: Organisms/strains		
LACB	Shanghai Model Organisms Center, Inc	N/A
LACP	Shanghai Model Organisms Center, Inc	N/A
Oligonucleotides		
Primers for genotyping	This paper	N/A
Recombinant DNA		
Plasmids for *prestin* genes	This paper	N/A
Software and algorithms		
PAML v4.7	https://doi.org/10.1093/molbev/msm088	http://abacus.gene.ucl.ac.uk/software/paml.html
GO.db v3.6.0	https://doi.org/10.18129/B9.bioc.GO.db	https://www.bioconductor.org/packages/3.6/data/annotation/html/GO.db.html
convCalScript v0.3	https://doi.org/10.1093/molbev/msv091	https://github.com/ztzou/conv_cal
GraphPad Prism 7.0	GraphPad Software Inc.	https://www.graphpad.com

RESOURCE AVAILABILITY

Lead contact

Further information and requests for resources and reagents should be directed to and will be fulfilled by the lead contact, Peng Shi (ship@mail.kiz.ac.cn).

Materials availability

This study did not generate new unique reagents.

Data and code availability

- The original code is available for download at https://github.com/shuifeng1988/Bats_echolocation_origin.

- This study did not generate raw sequence data.
- Any additional information required to reanalyze the data reported in this paper is available from the lead contact upon request.

EXPERIMENTAL MODEL AND SUBJECT DETAILS

In this study, Human embryonic kidney 293 (HEK293) cells were used as *in vitro* models. Gene synthesis, cell culture, and transient transfection were described in the Method details.

Animals

Two lines of transgenic mice were purchased from Shanghai Model Organisms Center, Inc. (Shanghai, China). All C57BL/6 mice were ensured sex balance and the 8-10-week old during the experiments. Animal care, procedures, and experimental protocols corresponded to national and institutional guidelines and were reviewed and approved by the Ethics Committee of the Kunming Institute of Zoology, Chinese Academy of Sciences. Mice were kept according to the national guidelines for animal care in a specifically pathogen-free animal facility. All efforts were made to minimize the number of animals used and their suffering.

METHOD DETAILS

Identification of molecular convergences of protein-coding genes across 27 mammals

The alignments of one-to-one orthologous protein-coding genes across 27 mammals were downloaded from the OrthoMaM database (Scornavacca et al., 2019), including three non-laryngeally echolocating fruit bats (*Pteropus alecto*, *Pteropus vampyrus*, and *Rousettus aegyptiacus*), two laryngeally echolocating rhinolophid bats (*Hipposideros armiger* and *Rhinolophus sinicus*) and five laryngeally echolocating yangochiropteran bats (*Myotis brandtii*, *Myotis lucifugus*, *Myotis davidii*, *Eptesicus fuscus*, *Miniopterus natalensis*). These non-bat mammals were chosen primarily due to their relatively close phylogenetic relationship with bats, their representativeness in major mammalian clades, and the high quality of their genomes (Sanger sequencing: $\geq$ 6×; Illumina sequencing: $\geq$ 100×). In addition, we also considered the balance of evolutionary comparisons. To date, there are several published high-quality genomes of echolocating toothed whales, but only one such genome of the nonecholocating baleen whale (*Balaenoptera acutorostrata*). To ensure a balanced comparison, we only included the bottlenose dolphin (*Tursiops truncatus*) as a representative of toothed whales. To ensure the reliability of our analyses and involve as many one-to-one orthologous protein-coding genes as possible, we required that the dataset at least included dolphin, minke whale, two of three Old World fruit bats, one of two rhinolophid bats, and three of the five yangochiropteran bats. Finally, we obtained 11,145 one-to-one orthologous protein-coding genes.

For every gene in the dataset, we inferred the ancestral protein sequence for each interior node of the phylogeny respectively using the maximum likelihood and the maximum parsimony methods (Yang, 2007). Then we counted the numbers of the convergent sites (C_{site}) and divergent sites (D_{site}) between dolphin (branch I) and each of the main ancestral branches of bats (branches III, IV, V, VI, VII, and VIII). Following the previous standards (Liu et al., 2018), we ensured the reliability of identifying the convergent and divergent sites by only considering the inferred ancestral amino acids with $\geq$0.95 posterior probabilities to determine convergent and divergent substitutions. Moreover, we discarded convergent and divergent sites within the poorly aligned fragments. If the mean pair-wise sequence similarity of $\pm$ 10 amino acids from a convergent or divergent site was lower than 70% or its lowest similarity was lower than 35%, this fragment was defined as a poorly aligned fragment. Although some valid convergent substitutions that happen to be flanked by poorly sequenced regions might be excluded, it is expected to have little impact on our analyses because the same criteria were also used for the control branch pairs. In addition, we examined the status of the identified convergent amino acids across 10 bat extant bat species and further confirmed that the convergent substitutions at these sites unlikely occurred within individual bats but on the examined ancestral bat branches. Here, a convergent substitution refers to a change from the same or different ancestral amino acid to the same descendant amino acid along phylogenetically distant branches, whereas a divergent substitution refers to a change resulting in the different descendant amino acid. If a gene contains at least one convergent site, it is defined as a convergent gene. As controls, we also identified convergent and divergent sites between the minke whale (branch II) and each of the main ancestral branches of bats (branches III, IV, V, VI, VII, and VIII), as well as between cow (branch II') and each of the main ancestral branches of bats (branches III, IV, V, VI, VII, and VIII).

Convergent evolution in hearing-related genes

We obtained annotations for each of 11,145 orthologous protein-coding genes by searching the Gene Ontology (GO) database from the *R* package GO.db (v 3.6.0). If a gene belongs to the GO term "sensory perception of sound (GO:0007605)," it was defined as a hearing-related gene. We finally identified a total of 104 hearing-related genes and the remaining ones were considered as nonhearing genes. The ratios of C_{site} to D_{site} were then calculated for the sets of hearing and nonhearing genes, respectively.

Neutrally expected molecular convergences

The expected value of C_{site} under neutral evolution for each one-to-one orthologous protein-coding gene was estimated based on the JTT-f_{site} substitution model by following a previous method (Zou and Zhang, 2015a). And then the expected values of C_{site} for the sets of hearing and nonhearing genes were the sums of the expected values from all 104 hearing-related and all nonhearing genes, respectively. Fisher's exact test was used to investigate whether the ratio of the number of observed convergent sites to that of expected convergent sites in hearing-related genes is significantly different from that in nonhearing genes for each of the comparisons.

Identification of molecular convergences of protein-coding genes across 116 mammals

We collected 10,866 one-to-one orthologous protein-coding genes across 116 mammals from the OrthoMaM database (v10b). Although each protein alignment did not always contain all of these species, it at least included four of five toothed whales in the database. Using the maximum likelihood approach and the criteria above, we identified the convergent and divergent sites in both hearing-related and nonhearing genes between toothed whales and the ancestral branch of all bats, as well as between toothed whales and other ancestral branches of bats.

Gene synthesis, cell culture, and transient transfection

The protein-coding region of *prestin* genes from the main ancestral bat branches, including the last common ancestor of bats (LCAB), the LCA of yinpterochiropteran bats, the LCA of yangochiropteran bats (LCAY), the LCA of rhinolophoid bats (LCAR), the LCA of pteropodid bats (LCAP), and the LCA of rhinolophid bats (LCAC), were inferred based on the phylogenetic tree of 40 mammals with *prestin* sequences using the above method (Liu et al., 2014). The inferences were reliable because the mean posterior probabilities for the entire protein exceeded 95% for these nodes. The inferred prestin sequence of LCAB was the same as that of the LCA of yinpterochiropteran bats. The prestin protein alignment of 40 mammals, as well as the inferred ancestral bats, was deposited in the Mendeley Data Search database (https://doi.org/10.17632/67r72zcfxx.2). The inferred prestin protein-coding sequences were synthesized (Generay, Shanghai, CN) and cloned into the expression vector pEGFP-N1 (Clontech), yielding C-terminal GFP fusion constructs. Further sequencing analyses were conducted to verify the correct orientation and reading frame for each of these constructs. Human embryonic kidney 293 (HEK293) cells were cultured in DMEM with 10% fetal bovine serum. When the cell confluence reached roughly 50-60% of the surface area of the dishes, the ancestral prestin and pEGFP-N1 fusion constructs (3 μg) were accomplished using Lipofectamine 2000 transfection reagent (10 μL; Invitrogen). After 24 - 48 hours of incubation, the successfully transfected cells were used for voltage-dependent nonlinear capacitance (NLC) measurements.

Electrophysiological experiments for NLC measurements

The whole-cell recording was used to measure NLC at room temperature (22 - 26°C) with EPC10 amplifiers (HEKA Instruments Inc.). Recording pipettes were pulled with resistances of 2.5 to 4 MΩ and were filled with an internal solution that consisted of (mM): 140 CsCl, 2 $MgCl_2$, 10 EGTA, and 10 HEPES at pH 7.2. The extracellular solution had the following composition (mM): 120 NaCl, 20 TEA-Cl, 2 $CoCl_2$, 2 $MgCl_2$, 10 HEPES, and 5 glucose at pH 7.2. Glucose was used to adjust osmolarity to 300 - 320 mOsm/L. The whole-cell membrane capacitance (C_m) was measured by the sine+DC software in Patchmaster with the voltage ramps ranging from −120 to +70 mV. The stimulus from the amplifier was close to 5 kHz. NLC was deduced by recording C_m and plotted against membrane potential (V_m). We assessed the voltage-dependent NLC by recording C_m during voltage ramps with a slope of 0.16 V/s and plotted C_m as a function of membrane potential (V_m). NLC data were fitted with the derivative of Boltzmann function:

$$C_m = \frac{Q_{max}\alpha}{\exp\left[\alpha\left(V_m - V_{1/2}\right)\right]\left(1+\exp\left[-\alpha\left(V_m - V_{1/2}\right)\right]\right)^2} + C_{lin}$$

where Q_{max} is the maximum charge transfer, $V_{1/2}$ is the voltage at which the maximum charge is equally distributed across the membrane, C_{lin} is the linear capacitance, and α is the slope factor of the voltage dependence of the charge transfer. We normalized the NLC by the linear capacitance of the cells due to different cells with different levels of prestin expression as a function of cell size. Because differences in Q_{max} could have been caused by cell size, the charge movement was normalized to C_{lin}, which is designated as charge density with the unit of fC/pF.

Generation of transgenic mice

The knock-in fragment containing the LACB or LACP prestin protein-coding sequences was ligated into the donor vector to create the construct LACB or LACP Prestin-IRES-EGFP-polyA with a length of 3.269 kb 5′ homology arm and a length of 4.532 kb 3′ homology arm. The construct was injected into the fertilized eggs of C57BL/6J mouse strain with Cas9 mRNA and gRNA (5′-TGGTGAATAACTGCAGACCATGG-3′). The founders were mated with C57BL/6J mice and the offsprings were intercrossed for ≥5 generations to obtain the transgenic mice with correct homologous recombination. The primers used for genotyping are as follows: LACB-prestin knock-in mice: 5′-GACCAATCTTACCATCTTTCCTT-3′, 5′-TTGTCAGGCT GTTTTATTACGG-3′, and 5′-GACGGCAACTACAAGACC-3′; LACP-prestin knock-in mice: 5′-CGAGAAA TCCTCAGAGCCTAGAAC-3′, 5′-CTCCTGCTTGCCAGAAACCC-3′, and 5′-GATGACAGCGAATGGACC GA-3′. All related animal experiments were approved by the Ethics Committee of the Kunming Institute of Zoology, Chinese Academy of Sciences.

Acoustic testing

Mice were anesthetized with an intraperitoneal injection of sodium pentobarbital (30 mg/kg). Using a heating pad, the animal's body temperature was maintained at 37.5°C during the recordings in a soundproof room. All the testing sounds were delivered by MF1 loudspeakers (TuckerDavis Technologies, Alachua, FL, USA). All the measurement signals were recorded using BioSigRZ software and RZ6 hardware (Tucker-Davis Technologies, Alachua, FL, USA). For ABR measurements, a subdermal needle electrode was located over the skull vertex while the ground electrode was placed on a 1-2 mm incision ventroposterior in the external pinna. The loudspeaker was placed around 2 cm in front of the animal nose and delivered click or tone burst (4, 8, 16, 24, and 32 kHz) sound with 5-90 dB SPL (5 dB intervals) intensities. The ABR signals were amplified, filtered (100-1000 Hz), and averaged (256 times) to be stored for offline analysis. The hearing threshold was the minimum sound intensity at which averaged waveforms could be distinguished and we defined 95 dB SPL as statistical data points when there were no detective ABR waveforms at those frequencies stimulated by 90 dB SPL and less. For DPOAE measurements, the mouse ear canal was covered by a modified pipette tip and the cubic distortion product was measured in response to primary tones (f_1 and f_2) using an ER-10B+ microphone system (Etymotic, Elk Grove Village, IL, USA). The frequency ratio (f_2/f_1) was 1.2 and the centered-around frequencies were 8, 16, and 24 kHz. The sound intensity of f_1 (L1) was 80 dB SPL and the sound intensity of f_2 (L2) was 70 dB SPL. The level of the $2f_1–f_2$ DPOAE response at each centered frequency was calculated by averaging three the absolute values of the difference between the recorded amplitude at $2f_1–f_2$ frequency and the noise floor calculated by averaging the six frequency bins on either side of the $2f_1–f_2$ frequency.

Prestin exhibition of outer hair cells

The cochleae were removed from the animals killed by CO_2 inhalation. Temporal bones were fixed in 4% paraformaldehyde at 4°C overnight and then decalcified in 10% EDTA solution at room temperature for 3 days. The organ of Corti was microdissected from the decalcified cochleae. The tissues were mounted in an antifading mountant medium with DAPI (S2110, Solarbio). The confocal images of the GFP-positive OHCs that proportionally express *prestin* were taken by a 100× glycerin-immersion lens of the Nikon A1 microscope with maximum intensity projections of z-stacks.

QUANTIFICATION AND STATISTICAL ANALYSIS

After identifying convergent and divergent substitutions of protein-coding genes between different ancestral branches of bats and other lineages, two-tailed χ^2 tests were performed to evaluate the statistical significance in Figure 1. For the functional experiments *in vitro* and *in vivo*, we used two-tailed Student's *t*-tests to assess the significance of differences between two groups in Figures 2 and 3. We have described how to conduct these tests in the "Method details" section.